Measurements of the observed cross sections for $e^+e^- \to$ exclusive light hadrons containing $\pi^0\pi^0$ at $\sqrt{s} = 3.773$, 3.650 and 3.6648 GeV

M. Ablikim[1], J. Z. Bai[1], Y. Bai[1], Y. Ban[11], X. Cai[1], H. F. Chen[15], H. S. Chen[1], H. X. Chen[1], J. C. Chen[1], Jin Chen[1], X. D. Chen[5], Y. B. Chen[1], Y. P. Chu[1], Y. S. Dai[17], Z. Y. Deng[1], S. X. Du[1], J. Fang[1], C. D. Fu[14], C. S. Gao[1], Y. N. Gao[14], S. D. Gu[1], Y. T. Gu[4], Y. N. Guo[1], K. L. He[1], M. He[12], Y. K. Heng[1], J. Hou[10], H. M. Hu[1], T. Hu[1], G. S. Huang[1a], X. T. Huang[12], Y. P. Huang[1], X. B. Ji[1], X. S. Jiang[1], J. B. Jiao[12], D. P. Jin[1], S. Jin[1], Y. F. Lai[1], H. B. Li[1], J. Li[1], L. Li[1], R. Y. Li[1], W. D. Li[1], W. G. Li[1], X. L. Li[1], X. N. Li[1], X. Q. Li[10], Y. F. Liang[13], H. B. Liao[1b], B. J. Liu[1], C. X. Liu[1], Fang Liu[1], Feng Liu[6], H. H. Liu[1c], H. M. Liu[1], J. B. Liu[1d], J. P. Liu[16], H. B. Liu[4], J. Liu[1], R. G. Liu[1], S. Liu[8], Z. A. Liu[1], F. Lu[1], G. R. Lu[5], J. G. Lu[1], C. L. Luo[9], F. C. Ma[8], H. L. Ma[1], L. L. Ma[1e], Q. M. Ma[1], M. Q. A. Malik[1], Z. P. Mao[1], X. H. Mo[1], J. Nie[1], R. G. Ping[1], N. D. Qi[1], H. Qin[1], J. F. Qiu[1], G. Rong[1], X. D. Ruan[4], L. Y. Shan[1], L. Shang[1], D. L. Shen[1], X. Y. Shen[1], H. Y. Sheng[1], H. S. Sun[1], S. S. Sun[1], Y. Z. Sun[1], Z. J. Sun[1], X. Tang[1], J. P. Tian[14], G. L. Tong[1], X. Wan[1], L. Wang[1], L. L. Wang[1], L. S. Wang[1], P. Wang[1], P. L. Wang[1], W. F. Wang[1f], Y. F. Wang[1], Z. Wang[1], Z. Y. Wang[1], C. L. Wei[1], D. H. Wei[3], Y. Weng[1], N. Wu[1], X. M. Xia[1], X. X. Xie[1], G. F. Xu[1], X. P. Xu[6], Y. Xu[10], M. L. Yan[15], H. X. Yang[1], M. Yang[1], Y. X. Yang[3], M. H. Ye[2], Y. X. Ye[15], C. X. Yu[10], G. W. Yu[1], C. Z. Yuan[1], Y. Yuan[1], S. L. Zang[1g], Y. Zeng[7], B. X. Zhang[1], B. Y. Zhang[1], C. C. Zhang[1], D. H. Zhang[1], H. Q. Zhang[1], H. Y. Zhang[1], J. W. Zhang[1], J. Y. Zhang[1], X. Y. Zhang[12], Y. Y. Zhang[13], Z. X. Zhang[11], Z. P. Zhang[15], D. X. Zhao[1], J. W. Zhao[1], M. G. Zhao[1], P. P. Zhao[1], B. Zheng[1], H. Q. Zheng[11], J. P. Zheng[1], Z. P. Zheng[1], B. Zhong[9] L. Zhou[1], K. J. Zhu[1], Q. M. Zhu[1], X. W. Zhu[1], Y. C. Zhu[1], Y. S. Zhu[1], Z. A. Zhu[1], Z. L. Zhu[3], B. A. Zhuang[1], B. S. Zou[1]

(BES Collaboration)

[1] *Institute of High Energy Physics, Beijing 100049, People's Republic of China*
[2] *China Center for Advanced Science and Technology(CCAST), Beijing 100080, People's Republic of China*
[3] *Guangxi Normal University, Guilin 541004, People's Republic of China*
[4] *Guangxi University, Nanning 530004, People's Republic of China*
[5] *Henan Normal University, Xinxiang 453002, People's Republic of China*
[6] *Huazhong Normal University, Wuhan 430079, People's Republic of China*
[7] *Hunan University, Changsha 410082, People's Republic of China*
[8] *Liaoning University, Shenyang 110036, People's Republic of China*
[9] *Nanjing Normal University, Nanjing 210097, People's Republic of China*
[10] *Nankai University, Tianjin 300071, People's Republic of China*
[11] *Peking University, Beijing 100871, People's Republic of China*
[12] *Shandong University, Jinan 250100, People's Republic of China*
[13] *Sichuan University, Chengdu 610064, People's Republic of China*
[14] *Tsinghua University, Beijing 100084, People's Republic of China*
[15] *University of Science and Technology of China, Hefei 230026, People's Republic of China*
[16] *Wuhan University, Wuhan 430072, People's Republic of China*
[17] *Zhejiang University, Hangzhou 310028, People's Republic of China*

[a] *Current address: University of Oklahoma, Norman, Oklahoma 73019, USA*
[b] *Current address: DAPNIA/SPP Batiment 141, CEA Saclay, 91191, Gif sur Yvette Cedex, France*
[c] *Current address: Henan University of Science and Technology, Luoyang 471003, People's Republic of China*
[d] *Current address: CERN, CH-1211 Geneva 23, Switzerland*
[e] *Current address: University of Toronto, Toronto M5S 1A7, Canada*
[f] *Current address: Laboratoire de l'Accélérateur Linéaire, Orsay, F-91898, France*
[g] *Current address: University of Colorado, Boulder, CO 80309, USA*

By analyzing the data sets of 17.3, 6.5 and 1.0 pb^{-1} taken, respectively, at $\sqrt{s} = 3.773$, 3.650 and 3.6648 GeV with the BES-II detector at the BEPC collider, we measure the observed cross sections for $e^+e^- \to \pi^+\pi^-\pi^0\pi^0$, $K^+K^-\pi^0\pi^0$, $2(\pi^+\pi^-\pi^0)$, $K^+K^-\pi^+\pi^-\pi^0\pi^0$ and $3(\pi^+\pi^-)\pi^0\pi^0$ at the three energy points. Based on these cross sections we set the upper limits on the observed cross sections and the branching fractions for $\psi(3770)$ decay into these final states at 90% C.L..

I. INTRODUCTION

In the past thirty years, it is expected that almost all of the $\psi(3770)$ decay into $D\bar{D}$ meson pairs. However, the earlier published data [1] show that the $\psi(3770)$ production cross section exceeds the $D\bar{D}$ production cross section by about 38% [2]. Recently, CLEO Collaboration measured the cross section for $e^+e^- \to \psi(3770) \to$ non-$D\bar{D}$ to be $(-0.01 \pm 0.08^{+0.41}_{-0.30})$ nb [3]. However, by analyzing different data samples with different methods, BES Collaboration extracted the branching fraction for $\psi(3770) \to$ non$-D\bar{D}$ decay to be $(15 \pm 5)\%$ [4, 5, 6, 7, 8], which means that there may exist substantial non-$D\bar{D}$ final states in the $\psi(3770)$ decays, or there are some new structure or physics effects which may partially be responsible for the large non$-D\bar{D}$ branching fraction of the $\psi(3770)$ decays measured by the BES collaboration

[9, 10].

BES Collaboration found the first non$-D\bar{D}$ decay mode of $\psi(3770)$, i.e. $\psi(3770) \to J/\psi\pi^+\pi^-$ for the first time, and extracted the branching fraction for $\psi(3770) \to J/\psi\pi^+\pi^-$ to be $(0.34 \pm 0.14 \pm 0.09)\%$ [11, 12]. Latter, CLEO Collaboration confirmed the BES observation [13] and observed more $\psi(3770)$ exclusive non-$D\bar{D}$ decays, $\psi(3770) \to J/\psi\pi^0\pi^0$, $J/\psi\pi^0$, $J/\psi\eta$ [13], $\gamma\chi_{cJ}(J = 0, 1, 2)$ [14, 15] and $\phi\eta$ [16], etc. However, the sum of these measured branching fractions for $\psi(3770) \to$ exclusive non-$D\bar{D}$ decays is not more than 2%. BES and CLEO Collaborations have also made many efforts to search for $\psi(3770)$ exclusive charmless decays by comparing the cross sections for $e^+e^- \to$ exclusive light hadrons measured at the peak of $\psi(3770)$ and at some continuum energy points [17, 18, 19, 20, 21] [16, 22, 23].

In this Letter, we report another effort to search for $\psi(3770)$ exclusive charmless decays, which are performed by studying some processes containing $\pi^0\pi^0$ mesons in the final states with the same method as the one used in Refs. [19, 20, 21]. We measure the observed cross sections for $e^+e^- \to \pi^+\pi^-\pi^0\pi^0$, $K^+K^-\pi^0\pi^0$, $2(\pi^+\pi^-\pi^0)$, $K^+K^-\pi^+\pi^-\pi^0\pi^0$ and $3(\pi^+\pi^-)\pi^0\pi^0$ at $\sqrt{s} = 3.773$, 3.650 and 3.6648 GeV. Then, we set the upper limits on the observed cross sections and the branching fractions for $\psi(3770)$ decay into these final states at 90% C.L.. The data used in the analysis were taken at the center-of-mass energies $\sqrt{s} = 3.773$, 3.650 and 3.6648 GeV with the BES-II detector at the BEPC collider, corresponding to the integrated luminosities of 17.3, 6.5 and 1.0 pb^{-1}, respectively. In the Letter, we call, respectively, the three data sets as the $\psi(3770)$ resonance data, the continuum data 1 and the continuum data 2.

II. BES-II DETECTOR

The BES-II is a conventional cylindrical magnetic detector [24, 25] operated at the Beijing Electron-Positron Collider (BEPC). A 12-layer vertex chamber (VC) surrounding the beryllium beam pipe provides input to the event trigger, as well as coordinate information. A forty-layer main drift chamber (MDC) located just outside the VC yields precise measurements of charged particle trajectories with a solid angle coverage of 85% of 4π; it also provides ionization energy loss (dE/dx) measurements which are used for particle identification. Momentum resolution of $1.7\%\sqrt{1+p^2}$ (p in GeV/c) and dE/dx resolution of 8.5% for Bhabha scattering electrons are obtained for the data taken at $\sqrt{s} = 3.773$ GeV. An array of 48 scintillation counters surrounding the MDC measures the time of flight (TOF) of charged particles with a resolution of about 180 ps for electrons. Outside the TOF, a 12 radiation length, lead-gas barrel shower counter (BSC), operating in limited streamer mode, measures the energies of electrons and photons over 80% of the total solid angle with an energy resolution of $\sigma_E/E = 0.22/\sqrt{E}$ (E in GeV) and spatial resolutions of $\sigma_\phi = 7.9$ mrad and $\sigma_z = 2.3$ cm for electrons. A solenoidal magnet outside the BSC provides a 0.4 T magnetic field in the central tracking region of the detector. Three double-layer muon counters instrument the magnet flux return and serve to identify muons with momentum greater than 0.5 GeV/c. They cover 68% of the total solid angle.

III. EVENT SELECTION

The exclusive light hadron final states of $\pi^+\pi^-\pi^0\pi^0$, $K^+K^-\pi^0\pi^0$, $2(\pi^+\pi^-\pi^0)$, $K^+K^-\pi^+\pi^-\pi^0\pi^0$ and $3(\pi^+\pi^-)\pi^0\pi^0$ are studied by examining the different photon combinations from $\pi^+\pi^-\gamma_1\gamma_2\gamma_3\gamma_4$, $K^+K^-\gamma_1\gamma_2\gamma_3\gamma_4$, $2(\pi^+\pi^-)\gamma_1\gamma_2\gamma_3\gamma_4$, $K^+K^-\pi^+\pi^-\gamma_1\gamma_2\gamma_3\gamma_4$ and $3(\pi^+\pi^-)\gamma_1\gamma_2\gamma_3\gamma_4$, respectively. The π^0 mesons are reconstructed through the decay $\pi^0 \to \gamma\gamma$.

For each candidate event, it is required that there are at least two charged tracks to be well reconstructed in the MDC with good helix fits and at least four neutral tracks to be well reconstructed in the BSC. The charged track is required to have the polar angle satisfying $|\cos\theta| < 0.85$, and originate from the interaction region $V_{xy} < 2.0$ cm and $|V_z| < 20.0$ cm. Here, V_{xy} and $|V_z|$ are the closest approaches of the charged track in the xy plane and in the z direction.

The charged particles are identified by using the dE/dx and TOF measurements, with which the combined confidence levels CL_π and CL_K for pion and kaon hypotheses are calculated. The candidate charged tracks satisfying $CL_\pi > 0.001$ and $CL_K > CL_\pi$ are identified as pion and kaon, respectively.

The good photons are selected with the BSC measurements. They are required to satisfy the following criteria: the energy deposited in the BSC is greater than 50 MeV, the electromagnetic shower starts in the first 5 layers, the angle between the photon and the nearest charged track is greater than 22° [26] and the opening angle between the cluster development direction and the photon emission direction is less than 37° [26].

For each selected candidate event, there may be several different charged or neutral track combinations satisfying the above selection criteria for exclusive light hadron final states. Each combination is subjected to an energy-momentum conservative kinematic fit. Candidates with a fit probability larger than 1% are accepted. If more than one combination satisfies the selection criteria in an event, only the combination with the largest fit probability is retained.

At center-of-mass energy of 3.773 GeV, the events of $\psi(2S) \to (\gamma)J/\psi\pi^0\pi^0$, with $J/\psi \to e^+e^-$ or $J/\psi \to \mu^+\mu^-$ may be misidentified as the $\pi^+\pi^-\pi^0\pi^0$ final state due to misidentifying e^+e^- or $\mu^+\mu^-$ pair as $\pi^+\pi^-$ pair. We suppress these events by requiring the invariant mass of $\pi^+\pi^-$ combination from each selected $\pi^+\pi^-\pi^0\pi^0$ candidate event to be less than 3.0 GeV/c^2.

The $K^+K^-\pi^+\pi^-\pi^0\pi^0$ final state suffers more contaminations from $D\bar{D}$ decays than the other four modes. To

eliminate these contaminations, we exclude the events from $D\bar{D}$ decays by rejecting those in which the D and $\bar{D}$ mesons can be reconstructed in the decay modes of $D^0 \to K^-\pi^+\pi^0$ and $\bar{D}^0 \to K^+\pi^-\pi^0$ [27]. The residual contaminations from the other D meson decays are further removed based on Monte Carlo simulation.

IV. DATA ANALYSIS

For each $\gamma_1\gamma_2\gamma_3\gamma_4$ combination satisfying the above selection criteria, there are three possible photon combinations ($[\pi^0_{\gamma_1\gamma_2}\pi^0_{\gamma_3\gamma_4}]$, $[\pi^0_{\gamma_1\gamma_3}\pi^0_{\gamma_2\gamma_4}]$,$[\pi^0_{\gamma_1\gamma_4}\pi^0_{\gamma_2\gamma_3}]$) which may be reconstructed as $\pi^0\pi^0$ meson pairs. We calculate the invariant masses for the $\gamma_i\gamma_j$ and $\gamma_{i'}\gamma_{j'}$ combinations, $M_{\gamma_i\gamma_j}$ and $M_{\gamma_{i'}\gamma_{j'}}$($i$, j, i', $j' = 1$, or 2, or 3, or 4; $i < j$, $i' < j'$, $i < i'$ and $j < j'$) with the fitted momentum vectors from the kinematic fit. Figure 1 shows the scatter plot for $M_{\gamma_{i'}\gamma_{j'}}$ versus $M_{\gamma_i\gamma_j}$ of the candidates for the $\pi^+\pi^-\pi^0\pi^0$, $K^+K^-\pi^0\pi^0$, $2(\pi^+\pi^-\pi^0)$, $K^+K^-\pi^+\pi^-\pi^0\pi^0$ and $3(\pi^+\pi^-)\pi^0\pi^0$ final states selected from the data including the three possible combinations.

In Fig. 1, the cluster around the $\pi^0\pi^0$ signal region indicates the production of the process containing $\pi^0\pi^0$ mesons in the final state. In the following analysis, the mass window of $\pm 3\sigma_{M_{\gamma\gamma}}(\pm 60$ MeV/$c^2)$ around the π^0 nominal mass is taken as the π^0 signal region, where $\sigma_{M_{\gamma\gamma}}$ is the π^0 mass resolution determined by Monte Carlo simulation. In each figure, projecting the events with $M_{\gamma_{i'}\gamma_{j'}}$ in the π^0 signal region onto $M_{\gamma_i\gamma_j}$ axis, we obtain the distribution of the $\gamma_i\gamma_j$ invariant masses for each process as shown in Fig. 2. Fitting each of the $\gamma_i\gamma_j$ invariant mass spectra in Fig. 2 with a Gaussian function for the π^0 signal and a polynomial for the background yields the number $N^{\pi^0_{\gamma_i\gamma_j}}_{\rm obs}$ of the events for each process observed from each of the data sets. However, in each event, there may be more than one combination entering the $\gamma_i\gamma_j$ invariant mass spectra. The number $N^{\rm rc}$ of the repeated counting events in the observed number $N^{\pi^0_{\gamma_i\gamma_j}}_{\rm obs}$ of π^0s from the fit is subtracted from the number of $N^{\pi^0_{\gamma_i\gamma_j}}_{\rm obs}$. The number of $N^{\rm rc}$ is accounted via the number of $N^{\pi^0_{\gamma_i\gamma_j}}_{\rm obs}$, the number of the repeated counting events and the number of all the events in the π^0 signal region, as well as the repeated counting rate of the combinatorial background events which is estimated with the events in sideband region.

Using the number of events observed in a sideband region which is the mass window of ± 60 MeV/c^2 around 0.335 GeV/c^2 in the $\gamma'_i\gamma'_j$ invariant mass spectra, we can estimate the contributions of the combinatorial $\gamma_{i'}\gamma_{j'}$ background in the $\pi^0_{\gamma_{i'}\gamma_{j'}}$ signal region. We obtain the number of these contributions, $N^{\pi^0_{\gamma_i\gamma_j}}_{\rm sid}$, by normalizing the fitted number of π^0s observed in the sideband region. Here, the normalization factor is the ratio of the number of the background events in the signal region over the

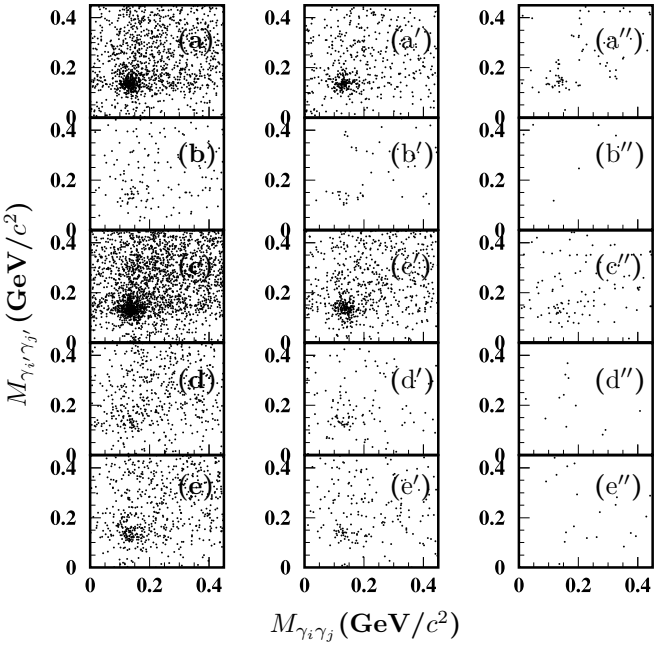

Fig. 1: The scatter plots of $M_{\gamma_{i'}\gamma_{j'}}$ versus $M_{\gamma_i\gamma_j}$ of the candidates for $e^+e^- \to$ (a) $\pi^+\pi^-\pi^0\pi^0$, (b) $K^+K^-\pi^0\pi^0$, (c) $2(\pi^+\pi^-\pi^0)$, (d) $K^+K^-\pi^+\pi^-\pi^0\pi^0$ and (e) $3(\pi^+\pi^-)\pi^0\pi^0$ selected from the $\psi(3770)$ resonance data (left), the continuum data 1 (middle) and the continuum data 2 (right).

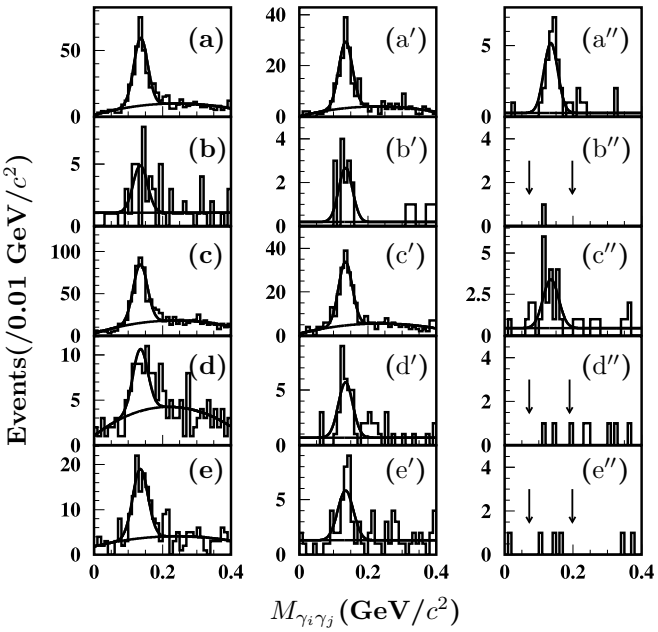

Fig. 2: The distributions of the invariant masses for the $\gamma_i\gamma_j$ combinations from the candidates for $e^+e^- \to$ (a) $\pi^+\pi^-\pi^0\pi^0$, (b) $K^+K^-\pi^0\pi^0$, (c) $2(\pi^+\pi^-\pi^0)$, (d) $K^+K^-\pi^+\pi^-\pi^0\pi^0$ and (e) $3(\pi^+\pi^-)\pi^0\pi^0$ from the $\psi(3770)$ resonance data (left), the continuum data 1 (middle) and the continuum data 2 (right), where the pairs of arrows show the π^0 signal region.

number of the background events in the sideband region.

However, there are only a few events in Fig. 2(b$''$), (d$''$) and (e$''$). Counting the events with $M_{\gamma\gamma}$ within the π^0 signal region, we obtain 1, 2 and 3 candidate events for $e^+e^- \to K^+K^-\pi^0\pi^0$, $K^+K^-\pi^+\pi^-\pi^0\pi^0$ and $3(\pi^+\pi^-)\pi^0\pi^0$ from the continuum data 2, respectively. In this case, we set the upper limit $N^{\rm up}$ on the number of the signal events at 90% confidence level (C.L.). Here, we use the Feldman-Cousins method [28] and ignore the background.

V. OTHER BACKGROUND SUBTRACTION

In Section IV, we have considered the combinatorial $\gamma\gamma$ background in the $\pi^0\pi^0$ reconstruction. However, there are still some other kinds of backgrounds from J/ψ and $\psi(3686)$ decays due to ISR returns, from the other final states due to the misidentification between charged pion and kaon, from the decays of $\psi(3770) \to J/\psi\pi^+\pi^-$, $J/\psi\pi^0\pi^0$, $J/\psi\pi^0$, $\gamma\chi_{cJ}$ ($J = 0, 1, 2$), and from $D\bar{D}$ decays. In order to directly compare the cross sections for $e^+e^- \to f$ (f represents exclusive light hadron final state) measured at the peak of $\psi(3770)$ and at some continuum energy points, we need to remove these background events. The method of background subtraction has been described in detail in Ref. [19]. Monte Carlo study shows that the contaminations from the decays of $\psi(3770) \to J/\psi\pi^+\pi^-$, $J/\psi\pi^0\pi^0$, $J/\psi\pi^0$ and $\psi(3770) \to \gamma\chi_{cJ}$ can be neglected [19] and the contaminations from the final states with an extra photon can be ignored.

For the process of $K^+K^-\pi^+\pi^-\pi^0\pi^0$, even though we have removed the main contaminations from $D\bar{D}$ decays in the previous event selection (see section III), there are still some residual contaminations from $D\bar{D}$ decays, which can satisfy the selection criteria for the $K^+K^-\pi^+\pi^-\pi^0\pi^0$ final state. The number of these residual contaminations are further removed based on Monte Carlo simulation.

Since we don't know the details about the resonance and the continuum amplitudes, we neglect the possible interference between them in the following analysis. In this case, by subtracting $N^{\rm rc}$, $N_{\rm sid}^{\pi^0_{\gamma_i\gamma_j}}$ and the number $N^{\rm b}$ of these contaminations from the number $N_{\rm obs}^{\pi^0_{\gamma_i\gamma_j}}$ of the candidate events, we obtain the net numbers $N^{\rm net}$ of the signal events for each process. The numbers of $N_{\rm obs}^{\pi^0_{\gamma_i\gamma_j}}$, $N^{\rm rc}$, $N_{\rm sid}^{\pi^0_{\gamma_i\gamma_j}}$, $N^{\rm b}$ and $N^{\rm net}$ (or $N^{\rm up}$) are summarized in Tabs. I, II and III.

VI. RESULTS

A. Monte Carlo efficiency

We estimate the detection efficiency ϵ for $e^+e^- \to f$ by using a phase space generator including initial state radiation and vacuum polarization corrections [29] with $1/s$ cross section energy dependence. Final state radiation [30] decreases the detection efficiency not more than 0.5%. The Monte Carlo events are generated based on the Monte Carlo simulation for the BES-II detector [31]. By analyzing these Monte Carlo events, we obtain the detection efficiency for each process at each center-of-mass energy. They are summarized in the fifth columns of Tabs. I, II and III. The detection efficiencies listed in the tables do not include the branching fraction for $\pi^0 \to \gamma\gamma$.

B. Observed cross sections

The observed cross section for $e^+e^- \to f$ is obtained by dividing the number $N^{\rm net}$ of the signal events by the integrated luminosity $\mathcal{L}$ of the data set, the detection efficiency ϵ and the square of the branching fraction $\mathcal{B}^2(\pi^0 \to \gamma\gamma)$ for $\pi^0 \to \gamma\gamma$,

$$\sigma_{e^+e^-\to f} = \frac{N^{\rm net}}{\mathcal{L} \times \epsilon \times \mathcal{B}^2(\pi^0 \to \gamma\gamma)}. \quad (1)$$

Inserting the numbers of $N^{\rm net}$, $\mathcal{L}$, ϵ and $\mathcal{B}(\pi^0 \to \gamma\gamma)$ in Eq. (1), we obtain $\sigma_{e^+e^-\to f}$ for each process at $\sqrt{s} = 3.773$, 3.650 and 3.6648 GeV, respectively. They are summarized in the last columns of Tabs. I, II and III, where the first error is statistical and the second systematic. The systematic error in the cross section measurement arises mainly from the uncertainties in integrated luminosity of the data set ($\sim 2.1\%$ [4, 5]), photon selection ($\sim 2.0\%$, per photon), tracking efficiency ($\sim 2.0\%$ per track), particle identification ($\sim 0.5\%$ per pion or kaon), kinematic fit ($\sim 1.5\%$), Monte Carlo statistics ($\sim (3.3 \sim 5.7)\%$), branching fraction quoted from PDG ($\sim 0.03\%$ for $B(\pi^0 \to \gamma\gamma)$), background subtraction ($\sim (0.0 \sim 6.1)\%$), fitting to the mass spectra ($\sim (2.4 \sim 9.5)\%$), and Monte Carlo modeling ($\sim 6.0\%$). Adding these uncertainties in quadrature yields the total systematic error $\Delta_{\rm sys}$ for each process at each center-of-mass energy.

C. Upper limits on the observed cross sections

The upper limits on the observed cross sections for $e^+e^- \to K^+K^-\pi^0\pi^0$, $K^+K^-\pi^+\pi^-\pi^0\pi^0$ and $3(\pi^+\pi^-)\pi^0\pi^0$ at $\sqrt{s} = 3.6648$ GeV are set by

$$\sigma^{\rm up}_{e^+e^-\to f} = \frac{N^{\rm up}}{\mathcal{L} \times \epsilon \times (1 - \Delta_{\rm sys}) \times \mathcal{B}^2(\pi^0 \to \gamma\gamma)}, \quad (2)$$

where $N^{\rm up}$ is the upper limit on the number of the signal events setting based on Feldman-Cousins method [28], and $\Delta_{\rm sys}$ is the systematic error in the cross section measurement. Inserting the numbers of $N^{\rm up}$, $\mathcal{L}$, ϵ, $\Delta_{\rm sys}$ and $\mathcal{B}(\pi^0\to\gamma\gamma)$ in Eq. (2), we obtain $\sigma^{\rm up}_{e^+e^-\to f}$ for these processes at $\sqrt{s}=3.6648$ GeV, which are also summarized in the last column of Tab. III.

D. Upper limits on the observed cross sections and the branching fractions for $\psi(3770)\to f$

In the $\psi(3770)$ resonance region [33], if we ignore the possible interference effects between the continuum and resonance amplitudes and the difference of the vacuum polarization corrections at $\sqrt{s}=3.773$ and 3.650 GeV, the contributions of the continuum production for $e^+e^-\to f$ at $\sqrt{s}=3.773$ GeV can be expected by these measured at $\sqrt{s}=3.650$ GeV. In this case, the observed cross section for $\psi(3770)\to f$ at $\sqrt{s}=3.773$ GeV can be written as

$$\sigma_{\psi(3770)\to f}=\sigma^{3.773\,{\rm GeV}}_{e^+e^-\to f}-f_{\rm co}\times\sigma^{3.650\,{\rm GeV}}_{e^+e^-\to f}, \qquad (3)$$

where $\sigma^{3.773\,{\rm GeV}}_{e^+e^-\to f}$ and $\sigma^{3.650\,{\rm GeV}}_{e^+e^-\to f}$ are the observed cross sections for $e^+e^-\to f$ measured at $\sqrt{s}=3.773$ and 3.650 GeV, respectively; $f_{\rm co}$ is the factor accounting for the $1/s$ dependence of the cross section. Neglecting the difference in the corrections for ISR and vacuum polarization effects at the two energy points, we have $f_{\rm co}=(3.650/3.773)^2$. With the $\sigma^{3.773\,{\rm GeV}}_{e^+e^-\to f}$ and $\sigma^{3.650\,{\rm GeV}}_{e^+e^-\to f}$ listed in Tabs. I and II, we determine $\sigma_{\psi(3770)\to f}$ at $\sqrt{s}=3.773$ GeV for each process. They are summarized in the second column of Tab. IV, where the first error is the statistical, the second is the independent systematic arising from the uncertainties in the Monte Carlo statistics, in the fit to the mass spectrum and in the background subtraction, and the third is the common systematic error arising from the other uncertainties as discussed in the subsection B.

Assuming that the cross section for $\psi(3770)\to f$ follows a Gaussian distribution, we set the upper limit on the observed cross section for $\psi(3770)\to f$ at $\sqrt{s}=3.773$ GeV, $\sigma^{\rm up}_{\psi(3770)\to f}$, which are summarized in the third column of Tab. IV.

The upper limit on the branching fraction $\mathcal{B}^{\rm up}_{\psi(3770)\to f}$ for $\psi(3770)\to f$ is set by dividing its upper limit on the observed cross section $\sigma^{\rm up}_{\psi(3770)\to f}$ by the observed cross section $\sigma^{\rm obs}_{\psi(3770)}=(7.15\pm0.27\pm0.27)$ nb [5, 19, 32] for the $\psi(3770)$ production at $\sqrt{s}=3.773$ GeV and a factor $(1-\Delta\sigma^{\rm obs}_{\psi(3770)})$, where $\Delta\sigma^{\rm obs}_{\psi(3770)}$ is the relative error of the $\sigma^{\rm obs}_{\psi(3770)}$. The results on $\mathcal{B}^{\rm up}_{\psi(3770)\to f}$ are summarized in the last column of Tab. IV.

VII. SUMMARY

In summary, by analyzing the data sets of 17.3, 6.5 and 1.0 pb^{-1} taken, respectively, at $\sqrt{s}=3.773$, 3.650 and 3.6648 GeV with the BES-II detector at the BEPC collider, we measured the observed cross sections for $e^+e^-\to\pi^+\pi^-\pi^0\pi^0$, $K^+K^-\pi^0\pi^0$, $2(\pi^+\pi^-\pi^0)$, $K^+K^-\pi^+\pi^-\pi^0\pi^0$ and $3(\pi^+\pi^-)\pi^0\pi^0$ at the three energy points. Based on the measured cross sections for these processes at $\sqrt{s}=3.773$ and 3.650 GeV, as well as the observed cross section for the $\psi(3770)$ production at $\sqrt{s}=3.773$ GeV, we also set the upper limits on the observed cross sections and the branching fractions for $\psi(3770)$ decay into these final states at 90% C.L.. These measurements provide useful experimental information for better understanding the possible excess of the cross section for the $\psi(3770)$ production relative to the cross section for the $D\bar{D}$ production and the mechanism of the continuum light hadron production.

VIII. ACKNOWLEDGMENTS

The BES collaboration thanks the staff of BEPC for their hard efforts. This work is supported in part by the National Natural Science Foundation of China under contracts Nos. 10491300, 10225524, 10225525, 10425523, the Chinese Academy of Sciences under contract No. KJ 95T-03, the 100 Talents Program of CAS under Contract Nos. U-11, U-24, U-25, the Knowledge Innovation Project of CAS under Contract Nos. U-602, U-34 (IHEP), the National Natural Science Foundation of China under Contract No. 10225522 (Tsinghua University).

[1] Particle Data Group, S. Eidelman *et al.*, Phys. Lett. B 592 (2004) 1.
[2] G. Rong, D. H. Zhang and J. C. Chen, hep-ex/0506051.
[3] CLEO Collaboration, D. Besson, *et al.*, Phys. Rev. Lett. 96 (2006) 092002.
[4] BES Collaboration, M. Ablikim *et al.*, Phys. Lett. B 641 (2006) 145.
[5] BES Collaboration, M. Ablikim *et al.*, Phys. Rev. Lett. 97 (2006) 121801.
[6] BES Collaboration, M. Ablikim *et al.*,
[7] BES Collaboration, M. Ablikim *et al.*, Phys. Rev. D 76 (2007) 122002.
[8] Particle Data Group, 2007 partial updata for edition 2008 (URL:http://pdg.lbl.gov).
[9] BES Collaboration, M. Ablikim *et al.*, Phys. Rev. Lett. 101 (2008) 102004.
[10] BES Collaboration, M. Ablikim *et al.*, Phys. Lett. B 668 (2008) 263.
[11] BES Collaboration, J. Z. Bai *et al.*, High Energy Physics and Nuclear Physics 28(4) (2004) 325.
[12] BES Collaboration, M. Ablikim *et al.*, Phys. Lett. B 605 (2005) 63.

[13] CLEO Collaboration, N. E. Adam *et al.*, Phys. Rev. Lett. 96 (2006) 082004.
[14] CLEO Collaboration, T. E. Coans *et al.*, Phys. Rev. Lett. 96 (2006) 182002.
[15] CLEO Collaboration, B. A. Briere *et al.*, Phys. Rev. D 74 (2006) 031106.
[16] CLEO Collaboration, D. Cronin-Hennessy *et al.*, Phys. Rev. D 74 (2006) 012005.
[17] BES Collaboration, M. Ablikim *et al.*, Phys. Rev. D 70, (2004) 077101.
[18] BES Collaboration, M. Ablikim *et al.*, Phys. Rev. D 72, (2005) 072007.
[19] BES Collaboration, M. Ablikim *et al.*, Phys. Lett. B 650 (2007) 111.
[20] BES Collaboration, M. Ablikim *et al.*, Phys. Lett. B 656 (2007) 30.
[21] BES Collaboration, M. Ablikim *et al.*, Eur. Phys. J. C 52 (2007) 805.
[22] CLEO Collaboration, G. S. Huang *et al.*, Phys. Rev. Lett. 96 (2006) 032003.
[23] CLEO Collaboration, G. S. Adams *et al.*, Phys. Rev. D 73 (2006) 012002.
[24] BES Collaboration, J. Z. Bai *et al.*, Nucl. Instrum. Methods A 344 (1994) 319.
[25] BES Collaboration, J. Z. Bai *et al.*, Nucl. Instrum. Methods A 458 (2001) 627.
[26] BES Collaboration, M. Ablikim *et al.*, Phys. Lett. B 597 (2004) 39.
BES Collaboration, M. Ablikim *et al.*, Phys. Lett. B 603 (2004) 130.
BES Collaboration, M. Ablikim *et al.*, Phys. Lett. B 608 (2005) 24.
[27] BES Collaboration, M. Ablikim *et al.*, Nucl. Phys. B 727 (2005) 395.
[28] G. J. Feldman and R. D. Cousins, Phys. Rev. D 57 (1998) 3873.
[29] E. A. Kuraev and V. S. Fadin, Yad. Fiz. 41 (1985) 377.
[30] E. Barberio and Z. Was, Comput. Phys. Commun. 79 (1994) 291.
[31] BES Collaboration, M. Ablikim *et al.*, Nucl. Instrum. Methods A 552 (2005) 344.
[32] BES Collaboration, M. Ablikim *et al.*, Phys. Lett. B 652 (2007) 238.
[33] Assuming that there is only one $\psi(3770)$ in the energy region from 3.70 to 3.87 GeV.

Tab. I: The observed cross sections for $e^+e^-\to$ exclusive light hadrons at $\sqrt{s}=3.773$ GeV, where $N^{\pi^0_{\gamma_i\gamma_j}}_{\rm obs}$ is the fitted number of events with $M_{\gamma_{i'}\gamma_{j'}}$ in the π^0 signal region observed from the $\psi(3770)$ resonance data, $N^{\rm rc}$ is the normalized number of the repeated counting events, $N^{\pi^0_{\gamma_i\gamma_j}}_{\rm sid}$ is the normalized number of events with $M_{\gamma_{i'}\gamma_{j'}}$ in the π^0 sideband region, $N^{\rm b}$ is the total number of the background events, $N^{\rm net}$ is the number of the signal events, ϵ is the detection efficiency, $\Delta_{\rm sys}$ is the relative systematic error in the cross section measurement, σ is the observed cross section.

$e^+e^-\to f$	$N^{\pi^0_{\gamma_i\gamma_j}}_{\rm obs}$	$N^{\rm rc}$	$N^{\pi^0_{\gamma_i\gamma_j}}_{\rm sid}$	$N^{\rm b}$	$N^{\rm net}$	$\epsilon(\%)$	$\Delta_{\rm sys}(\%)$	$\sigma^{\rm obs}$ [pb]
$\pi^+\pi^-\pi^0\pi^0$	259.7 ± 21.8	5.2 ± 7.2	29.8 ± 10.4	7.1 ± 2.2	217.6 ± 25.3	6.00 ± 0.21	13.0	$214.8\pm25.0\pm27.9$
$K^+K^-\pi^0\pi^0$	19.8 ± 5.6	0.0 ± 0.0	4.0 ± 3.1	2.0 ± 0.5	13.8 ± 6.4	3.06 ± 0.15	15.1	$26.7\pm12.4\pm4.0$
$2(\pi^+\pi^-\pi^0)$	374.6 ± 29.0	31.5 ± 10.6	29.2 ± 15.6	8.5 ± 1.4	305.4 ± 34.6	1.72 ± 0.07	14.1	$1051.5\pm119.2\pm148.3$
$K^+K^-\pi^+\pi^-\pi^0\pi^0$	38.2 ± 9.5	7.1 ± 4.3	0.7 ± 4.3	5.9 ± 1.5	24.5 ± 11.4	0.78 ± 0.03	16.8	$186.0\pm86.4\pm31.2$
$3(\pi^+\pi^-)\pi^0\pi^0$	81.2 ± 14.2	17.0 ± 5.1	2.4 ± 5.2	2.6 ± 0.7	59.2 ± 16.0	0.36 ± 0.02	18.5	$973.8\pm262.8\pm180.2$

Tab. II: The observed cross sections for $e^+e^-\to$ exclusive light hadrons at $\sqrt{s}=3.650$ GeV, where $N^{\pi^0_{\gamma_i\gamma_j}}_{\rm obs}$ is the fitted number of events with $M_{\gamma_{i'}\gamma_{j'}}$ in the π^0 signal region observed from the continuum data 1, and the definitions of the other symbols are the same as those in Tab. I.

$e^+e^-\to f$	$N^{\pi^0_{\gamma_i\gamma_j}}_{\rm obs}$	$N^{\rm rc}$	$N^{\pi^0_{\gamma_i\gamma_j}}_{\rm sid}$	$N^{\rm b}$	$N^{\rm net}$	$\epsilon(\%)$	$\Delta_{\rm sys}(\%)$	$\sigma^{\rm obs}$ [pb]
$\pi^+\pi^-\pi^0\pi^0$	132.6 ± 15.4	8.0 ± 2.8	6.6 ± 7.1	2.3 ± 0.8	115.7 ± 17.2	6.24 ± 0.23	13.5	$292.2\pm43.4\pm39.4$
$K^+K^-\pi^0\pi^0$	12.0 ± 3.9	0.0 ± 0.0	0.8 ± 1.4	1.0 ± 0.3	10.2 ± 4.2	2.96 ± 0.14	14.8	$54.3\pm22.1\pm8.0$
$2(\pi^+\pi^-\pi^0)$	147.6 ± 16.2	18.3 ± 8.6	8.7 ± 7.7	0.3 ± 0.2	120.3 ± 19.9	1.76 ± 0.07	15.3	$1077.3\pm178.1\pm164.8$
$K^+K^-\pi^+\pi^-\pi^0\pi^0$	25.7 ± 5.8	7.0 ± 2.6	0.7 ± 1.5	0.2 ± 0.1	17.8 ± 6.5	0.74 ± 0.03	15.1	$379.1\pm139.1\pm57.2$
$3(\pi^+\pi^-)\pi^0\pi^0$	25.7 ± 6.4	7.0 ± 2.6	0.0 ± 0.0	0.0 ± 0.0	18.7 ± 6.9	0.35 ± 0.02	19.1	$842.1\pm311.1\pm160.8$

Tab. III: The observed cross sections for $e^+e^-\to$ exclusive light hadrons at $\sqrt{s}=3.6648$ GeV, where $N^{\pi^0_{\gamma_i\gamma_j}}_{\rm obs}$ is the fitted number of events with $M_{\gamma_{i'}\gamma_{j'}}$ in the π^0 signal region observed from the continuum data 2, $N^{\rm up}$ is the upper limit on the number of the signal events, $\sigma^{\rm up}$ is the upper limit on the observed cross section set at 90% C.L., and the definitions of the other symbols are the same as those in Tab. I.

$e^+e^-\to f$	$N^{\pi^0_{\gamma_i\gamma_j}}_{\rm obs}$	$N^{\rm rc}$	$N^{\pi^0_{\gamma_i\gamma_j}}_{\rm sid}$	$N^{\rm b}$	$N^{\rm net}$ (or $N^{\rm up}$)	$\epsilon(\%)$	$\Delta_{\rm sys}(\%)$	$\sigma^{\rm obs}$ (or $\sigma^{\rm up}$) [pb]
$\pi^+\pi^-\pi^0\pi^0$	24.9 ± 5.3	1.0 ± 1.0	0.0 ± 0.0	0.4 ± 0.1	23.5 ± 5.4	6.06 ± 0.20	12.8	$397.3\pm91.3\pm50.9$
$K^+K^-\pi^0\pi^0$	1	-	-	-	<4.36	3.14 ± 0.14	12.0	<161.7
$2(\pi^+\pi^-\pi^0)$	16.9 ± 4.8	2.0 ± 1.4	0.0 ± 0.0	0.1 ± 0.1	14.8 ± 5.0	1.73 ± 0.06	13.9	$876.4\pm296.1\pm121.8$
$K^+K^-\pi^+\pi^-\pi^0\pi^0$	2	-	-	-	<5.91	0.77 ± 0.03	15.1	<926.2
$3(\pi^+\pi^-)\pi^0\pi^0$	3	-	-	-	<7.42	0.35 ± 0.02	17.2	<2623.1

Tab. IV: The upper limit on the observed cross section $\sigma^{\rm up}_{\psi(3770)\to f}$ at $\sqrt{s}=3.773$ GeV and the upper limit on the branching fraction $\mathcal{B}^{\rm up}_{\psi(3770)\to f}$ for $\psi(3770)\to f$ set at 90% C.L.. The $\sigma_{\psi(3770)\to f}$ in the second column is calculated with Eq. (3), where the first error is the statistical, the second is the independent systematic, and the third is the common systematic error.

Decay Mode	$\sigma_{\psi(3770)\to f}$ [pb]	$\sigma^{\rm up}_{\psi(3770)\to f}$ [pb]	$B^{\rm up}_{\psi(3770)\to f}$ [$\times10^{-3}$]
$\pi^+\pi^-\pi^0\pi^0$	$-58.6\pm47.7\pm25.7\pm6.5$	<61.1	<8.9
$K^+K^-\pi^0\pi^0$	$-24.1\pm24.1\pm5.8\pm2.7$	<28.9	<4.2
$2(\pi^+\pi^-\pi^0)$	$43.3\pm204.9\pm95.4\pm5.7$	<399.5	<58.5
$K^+K^-\pi^+\pi^-\pi^0\pi^0$	$-168.8\pm156.2\pm32.9\pm22.3$	<182.1	<26.7
$3(\pi^+\pi^-)\pi^0\pi^0$	$185.7\pm392.2\pm122.0\pm29.9$	<801.6	<117.4